Coordination of mRNA and tRNA methylations by TRMT10A

R. Jordan Ontiveros[a,b,1], Hui Shen[a,1], Julian Stoute[a,b], Amber Yanas[a,b], Yixiao Cui[a], Yuyu Zhang[a], and Kathy Fange Liu[a,b,2]

[a]Department of Biochemistry and Biophysics, Perelman School of Medicine, University of Pennsylvania, Philadelphia, PA 19104; and [b]Graduate Group in Biochemistry and Molecular Biophysics, Perelman School of Medicine, University of Pennsylvania, Philadelphia, PA 19104

Edited by Lynne E. Maquat, University of Rochester School of Medicine and Dentistry, Rochester, NY, and approved February 25, 2020 (received for review August 21, 2019)

The posttranscriptional modification of messenger RNA (mRNA) and transfer RNA (tRNA) provides an additional layer of regulatory complexity during gene expression. Here, we show that a tRNA methyltransferase, TRMT10A, interacts with an mRNA demethylase FTO (ALKBH9), both in vitro and inside cells. TRMT10A installs N^1-methylguanosine (m^1G) in tRNA, and FTO performs demethylation on N^6-methyladenosine (m^6A) and N^6,2′-*O*-dimethyladenosine (m^6A_m) in mRNA. We show that TRMT10A ablation not only leads to decreased m^1G in tRNA but also significantly increases m^6A levels in mRNA. Cross-linking and immunoprecipitation, followed by high-throughput sequencing results show that TRMT10A shares a significant overlap of associated mRNAs with FTO, and these mRNAs have accelerated decay rates potentially through the regulation by a specific m^6A reader, YTHDF2. Furthermore, transcripts with increased m^6A upon TRMT10A ablation contain an overrepresentation of m^1G9-containing tRNAs codons read by $tRNA^{Gln(TTG)}$, $tRNA^{Arg(CCG)}$, and $tRNA^{Thr(CGT)}$. These findings collectively reveal the presence of coordinated mRNA and tRNA methylations and demonstrate a mechanism for regulating gene expression through the interactions between mRNA and tRNA modifying enzymes.

tRNA | mRNA | modification

To date, about 150 types of RNA chemical modifications on almost all RNA species have been described (1–4). These modifications can dramatically expand the RNA alphabet by altering RNA structures, affinity to proteins, and base-pairing ability, greatly impacting how RNA influences the genetic flow of information from transcription to protein synthesis (2, 5–9). While many of the enzymes that deposit and remove RNA modifications have been identified, the details of how RNA modifications are regulated remain poorly understood.

Among those RNA species, transfer RNA (tRNA) is the most extensively modified. tRNA methylations are known to be critical for their stability and translational fidelity (1, 10, 11). TRMT10A is an *S*-adenosylmethionine–dependent methyltransferase that installs N^1-methylguanosine (m^1G) in tRNAs at the ninth position. While previous studies have identified the m^1G9 sites in tRNAs in human cells (12, 13), TRMT10A is, so far, the only known methyltransferase that installs this modification in human tRNA. The entire substrate repertoire of TRMT10A in human cells has not been fully revealed, although $tRNA^{Gln}$ and $tRNA^{iMet}$ were shown as the substrates of human TRMT10A in pancreatic β-cells (14). Previous efforts in characterizing the tRNA substrates of TRMT10A were mostly done in yeast (15–17). Human TRMT10A was shown installing m^1G9 in tRNAs in vitro using yeast and human tRNAs as the substrates (18). Mutations in TRMT10A have been observed in patients with young-onset diabetes syndrome and primary microcephaly-mild intellectual disability (14, 19–22), and recent studies have suggested that deficiency of TRMT10A can induce apoptosis in pancreatic cells, consistent with the correlation with diabetes (14, 22). However, the mechanism by which deficiency of TRMT10A is linked to the disease phenotype remains enigmatic.

Another major type of RNA, messenger RNA (mRNA), also carries methylations. The most prevalent internal modification in mRNA is N^6-methyladenosine (m^6A), which impacts nearly every step of RNA processing, including reducing or extending RNA half-life in cells (23–28). The methyltransferase heterodimer complex of METTL3 and METTL14 installs m^6A in mRNA (29–32). ALKBH5 and FTO (also known as ALKBH9) are the only known m^6A demethylase enzymes (33, 34). FTO can also remove N^6,2′-*O*-dimethyladenosine (m^6A_m) in mRNA (35, 36), and it is thus most appropriately referred to as an m^6A/m^6A_m demethylase. FTO was also reported performing demethylation on m^1A in mRNA and tRNA (37). The substrate selectivity of FTO has been suggested to be dependent on its predominant subcellular localization (37). The removal of m^6A by FTO can lead to differential regulation by m^6A readers, which specifically recognize the modification sites and bridge them to specific cellular complexes, such as the splicing complex, translational machinery, and RNA decay machinery (25, 27, 38–42). Thus far, a handful of m^6A readers have been identified that all specifically recognize m^6A in mRNA, and yet can lead to different or even opposite cellular consequences

Significance

It has been demonstrated that a diverse set of enzyme-mediated chemical modifications are found within RNAs, and these modifications markedly influence the fate of RNAs in cells. Dysregulation of such RNA modifications is involved in the development of a battery of human disorders. Studies to date have focused solely on individual modifications on isolated RNA; however, RNA modifications exist concurrently in multiple RNA species. Using biochemistry and high-throughput sequencing techniques, we revealed an interaction between a transfer RNA methyltransferase TRMT10A and a messenger RNA demethylase FTO, which influences the methylation levels on a subset of messenger RNAs. This study unravels a regulatory mechanism by which methylations across distinct RNA types are coordinated to impact gene expression collaboratively.

Author contributions: H.S. and K.F.L. designed research; R.J.O., H.S., J.S., A.Y., Y.C., Y.Z., and K.F.L. performed research; H.S., J.S., and K.F.L. analyzed data; and R.J.O., H.S., and K.F.L. wrote the paper.

The authors declare no competing interest.

This article is a PNAS Direct Submission.

Data deposition: The data reported in this paper have been deposited in the Gene Expression Omnibus (GEO) database, https://www.ncbi.nlm.nih.gov/geo (accession number GSE146207).

[1]R.J.O. and H.S. contributed equally to this work.

[2]To whom correspondence may be addressed. Email: liufg@pennmedicine.upenn.edu.

This article contains supporting information online at https://www.pnas.org/lookup/suppl/doi:10.1073/pnas.1913448117/-/DCSupplemental.

First published March 25, 2020.

(43–46). The functional significance of RNA-modifying enzymes and reader proteins is further evidenced by the fact that dysregulation of mRNA modification status or mutations in RNA-modifying enzymes has been linked to a battery of human diseases, including cancer, neurodegenerative disease, and diabetes (47–51).

Interestingly, previous studies have identified a few RNA-modifying enzymes that can install the same modification in different RNA species (52). For example, tRNA splicing ligase also acts as a ligase for noncanonical mRNA splicing. Additionally, tRNA pseudouridine synthases modify mRNAs (53–55). In addition, the yeast tRNA methyltransferase Trm140 has been shown to modify a noncanonical tRNA target only when associated with a seryl-tRNA synthetase (56). Considering these examples of noncanonical substrate targeting by putatively type-specific enzymes, it is not surprising that FTO itself has been reported to perform its demethylation activity on both tRNAs and mRNAs (37). Furthermore, there are examples of the unusual collaboration of RNA modifications by proteins not possessing modification activity (56) and coordination between tRNA modifications and gene transcription (57). These studies hint at an unusual mode of RNA modification regulation whereby the activity and selectivity of type-specific RNA-modifying enzymes can change upon association with a partner protein. It stands to reason that the regulation of two separate RNA modifications and two separate RNA species can be bridged together to regulate gene expression.

Despite the general acceptance that modifications in both mRNA and tRNA are indispensable for the precise regulation and coordination of gene expression, studies to date have focused solely on the modification status of the individual types of RNA species, as opposed to understanding how the modification status across multiple RNA species is collectively regulated or coordinated. Here, we describe a connection between the methylation status of mRNA and tRNA in the regulation of gene expression. We discovered that the tRNA m^1G methyltransferase TRMT10A and the mRNA m^6A/m^6A_m demethylase FTO interact with each other. Strikingly, TRMT10A ablation impacts not only the level of m^1G in tRNA but also m^6A levels in mRNA. The RNA half-life was examined across the overlapped targets of FTO and TRMT10A. Finally, thorough analyses of codon usage were executed on transcripts with increased m^6A peaks upon TRMT10A ablation. These experiments collectively suggest that the tRNA methyltransferase TRMT10A not only regulates m^1G levels in tRNA but also exhibits a dual function in tuning the activity and selectivity of the mRNA demethylase FTO. In turn, FTO with modified activity affects m^6A levels in mRNA, leading to downstream effects on gene expression.

Results

TRMT10A Interacts with m^6A/m^6A_m Demethylase Enzyme FTO. To identify the proteins associated with TRMT10A, we first constructed an HEK293T cell line stably expressing a tagged TRMT10A (N-terminal FLAG and HA tags in tandem) (*SI Appendix*, Fig. S1*A*) and used tandem-affinity purification of the FLAG-HA–tagged TRMT10A followed by protein mass spectrometry (TAP-MS) to identify TRMT10A-associated proteins. A control sample stably expressing FLAG-HA peptide without TRMT10A was processed in parallel (*SI Appendix*, Fig. S1*B*). These experiments were carried out with nuclear lysate because TRMT10A is primarily located in the cell nucleus (22). The TAP-MS analyses suggested that the potential associated proteins of TRMT10A in the nucleus are involved in carbon metabolism, glycolysis regulation, and DNA damage repair (*SI Appendix*, Fig. S1 *B* and *C* and Dataset S1), consistent with the previously reported function of TRMT10A as a tRNA m^1G methyltransferase linked to the regulation of RNA processing and energy metabolism (*SI Appendix*, Fig. S1*C*).

An unexpected, yet interesting observation is that many proteins identified from the TAP-MS experiments are involved in the regulation of mRNA methylation status, including the m^6A demethylase FTO (Dataset S1). These results led us to investigate if TRMT10A is involved in the regulation of both mRNA and tRNA methylations. Hence, further characterizations of this potential interaction were executed. To validate the protein–protein interactions between FTO and TRMT10A by an independent technique, we performed immunoprecipitation experiments with endogenous TRMT10A as the bait protein followed by Western blot. TRMT10A is shown in Fig. 1*A* interacting with FTO in an RNA-facilitated manner. Adding Rnase A led to decreased binding between FTO and TRMT10A; however, it did not abolish their interactions. Reciprocally, we performed the reverse immunoprecipitation using endogenous FTO to pull down TRMT10A. As shown in Fig. 1*B*, endogenous FTO pulled down TRMT10A. These experiments were reproducible with two TRMT10A antibodies and two FTO antibodies (*SI Appendix*, Fig. S2 *A* and *B*). In addition, we showed that FLAG-tagged TRMT10A can pull down FTO and FLAG-tagged FTO can reciprocally pull down TRMT10A (*SI Appendix*, Fig. S2 *C* and *D*). Furthermore, we carried out proximity ligation assays (PLA) to investigate the in situ interactions between FTO and TRMT10A. As shown in Fig. 1*C*, we observed fluorescence puncta in wild-type HEK 293T cells by using an anti-TRMT10A antibody and an anti-FTO, antibody, which recognize endogenous TRMT10A and FTO, respectively. We observed similar results when we used anti-FTO and anti-FLAG (recognizing FLAG-tagged TRMT10A) antibodies. In contrast, there were negligible fluorescence signals when we performed PLA in TRMT10A knockout cells (Fig. 1*B*), matching the signal from the cells that were not treated with any primary antibodies or only secondary probes but with no antibodies administered (*SI Appendix*, Fig. S3). To test if the self-oligomerization of primary antibodies produced false-positive signals, we performed single-recognition PLAs using a serial titration of each primary antibody and observed negligible false-positive signals (*SI Appendix*, Fig. S3). Next, we employed an in vitro GST pull-down experiment using purified full-length GST–TRMT10A fusion protein and purified full-length His_6-tagged FTO. As shown in *SI Appendix*, Fig. S4, His_6-FTO and GST–TRMT10A were each purified to near homogeneity. Initial experiments revealed that TRMT10A can pull down FTO directly (Fig. 1*D*). We further added purified polyadenylated RNA in the pull-down experiments. The results showed that the presence of polyadenylated RNA strengthens the association between FTO and TRMT10A (Fig. 1*D*). Finally, we examined whether TRMT10A interacts with the other mRNA m^6A demethylase, ALKBH5. The result of immunoprecipitation and PLA assays both showed no interaction between ALKBH5 and TRMT10A (*SI Appendix*, Fig. S5). These data together suggest that the interaction between TRMT10A and FTO is specific.

TRMT10A Indirectly Influences mRNA m^6A Levels in Addition to Its Canonical tRNA m^1G Methyltransferase Activity. Since TRMT10A interacts with the m^6A/m^6A_m demethylase FTO, we examined whether TRMT10A, a tRNA m^1G methyltransferase, can influence the level of m^6A in mRNA through its interaction with FTO. First, we performed TRMT10A transient knockdown, reaching a knockdown efficiency of 85% (*SI Appendix*, Fig. S6*A*). We also obtained four single-colony *TRMT10A* knockout HEK293T cell lines using CRISPR/Cas9 (*SI Appendix*, Fig. S6*B*).

To analyze the m^6A levels in polyadenylated RNAs from TRMT10A knockdown versus knockdown control as well as *TRMT10A* knockout versus wild-type samples, we first purified polyadenylated RNAs by performing two rounds of poly-dT extraction followed by ribominus treatment to obtain pure polyadenylated RNAs (*SI Appendix*, Fig. S7). We analyzed the m^6A/A

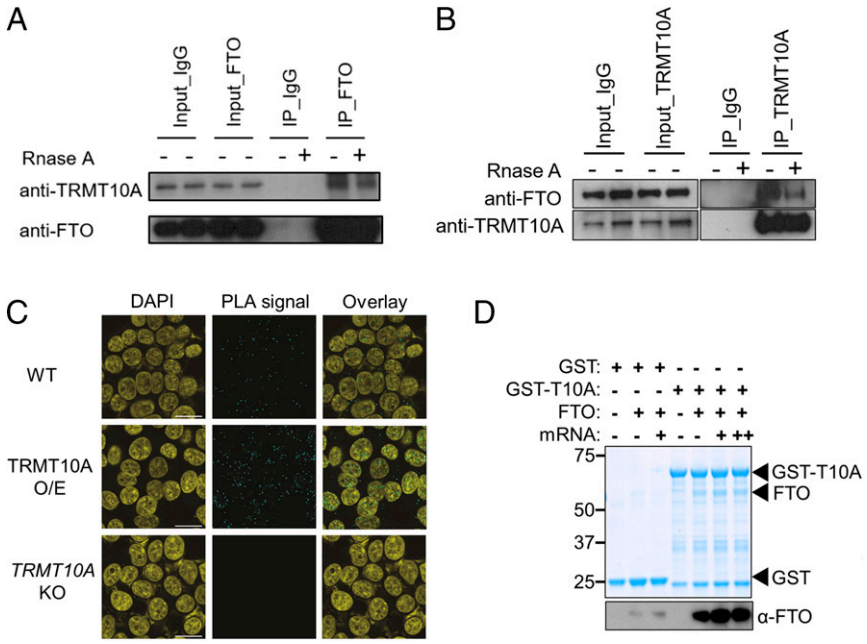

Fig. 1. TRMT10A interacts with mRNA m^6A/m^6A_m demethylase FTO. Western blot showing that (*A*) TRMT10A immunoprecipitated with FTO and (*B*) FTO immunoprecipitated with TRMT10A in an RNA-facilitated manner in HEK293T cells. The input and immunoprecipitation (IP) were from the same Western blot but taken under two exposure times. (*C*) PLA imaging showing that FTO interacts with TRMT10A in situ in HEK293T cells. (*Top*) Anti-FTO and anti-TRMT10A antibodies were administrated in wild-type HEK293T cells. (*Middle*) Anti-FTO and anti-flag antibodies were administrated in TRMT10A stable expression cells. (*Bottom*) Anti-FTO and anti-TRMT10A antibodies were administrated in *TRMT10A* knockout (KO) cells. Nuclei were stained with DAPI. PLA interaction signals are shown as cyan puncta (Scale bars, 20 nm.) (*D*) TRMT10A directly associates with FTO, as shown by GST-pulldown experiments. To validate the protein pulled down by GST-fusion TRMT10A, we performed immunoblot with an anti-FTO antibody.

ratio in these purified polyadenylated RNAs by LC-MS/MS quantification. The results showed that knockdown of TRMT10A leads to a significant increase of m^6A in the polyadenylated RNA species in comparison to the control sample. Increased m^6A levels were observed in the polyadenylated RNAs from all of the four *TRMT10A* knockout cell lines in comparison with the control (Fig. 2 *A* and *B* and *SI Appendix*, Figs. S8 and S9*A*). We employed knockdown of ALKBH5 as a positive control. As shown in *SI Appendix*, Fig. S9 *B* and *C*, knockdown of ALKBH5, leads to an obvious increase in m^6A level in polyadenylated-RNA in comparison with the knockdown control.

We also performed dot-blot assays and m^6A fluorescence immunostaining on *TRMT10A* knockout cell lines in comparison to the wild-type cells. To ensure the specificity of the anti-m^6A antibodies from two commercial vendors, we incubated the antibodies with in vitro-transcribed RNA oligos containing either m^6A, N^1-methyladenosine (m^1A), or unmodified adenosine. The results showed that the m^6A antibodies from both commercial vendors react exclusively with the m^6A-containing RNA probe but not with the m^1A-containing RNA probe or with the unmodified adenosine (*SI Appendix*, Fig. S10 *A* and *B*). We then used the validated m^6A antibodies in the m^6A fluorescence immunostaining and the dot-blot assays to examine the level of m^6A in different samples. The results consistently showed that *TRMT10A* knockout leads to increased m^6A (Fig. 2 *C* and *D* and *SI Appendix*, Fig. S10*C*). To examine whether the changes in m^6A levels were specifically linked to the deficiency of TRMT10A and not to other methyltransferases, we chose a tRNA methyltransferase NSUN2 and an rRNA methyltransferase NSUN5 as controls to conduct parallel knockdown experiments. We performed NSUN2 knockdown and NSUN5 knockdown, respectively, and compared the m^6A/A levels in mRNA from the knockdown samples to their control samples. LC-MS/MS results showed that knockdown of NSUN2 or NSUN5 do not lead to m^6A level changes in mRNA (*SI Appendix*, Fig. S11). The results confirmed that the effects on m^6A in poly(A) RNA are specific to TRMT10A rather than a universal effect resulting from the ablation of any RNA methyltransferase. In addition, the LC-MS/MS results showed no obvious changes in m^6A levels in 18S rRNA and 28S rRNA between TRMT10A knockdown and the knockdown control cells, as well as *TRMT10A* knockout versus wild-type cells (*SI Appendix*, Fig. S12). There is a slight (not statistically significant) increased level of m^6A in RNA smaller than 200 nucleotides upon TRMT10A ablation; however, the difference is not comparable to the level changes we observed in poly(A)-RNA (*SI Appendix*, Fig. S12).

Considering that FTO has been previously shown to remove m^6A_m in mRNA, we quantified the levels of m^6A_m in polyadenylated RNAs extracted from TRMT10A knockdown in comparison to the knockdown control, as well as *TRMT10A* knockout in comparison to the wild-type cells. The results showed that neither knockdown nor knockout of *TRMT10A* leads to noticeable changes in m^6A_m in mRNA (*SI Appendix*, Fig. S13). Our results suggest that the association of FTO and TRMT10A influences the level of mRNA m^6A rather than m^6A_m in HEK 293T cells.

TRMT10A Deficiency Positively Influences Transcriptome-Wide m^6A Deposition in mRNA. Considering the increased m^6A levels in polyadenylated RNAs upon TRMT10A ablation and the fact that our TAP-MS, coimmunoprecipitation, immunoblotting, PLA assays, and GST-pulldown experiments suggested that TRMT10A interacts with FTO (Figs. 1 and 2 and *SI Appendix*, Fig. S2), we next sought to identify the transcripts containing TRMT10A-sensitive m^6A sites.

To answer this question, we carried out transcriptome-wide m^6A-sequencing (m^6A-seq) experiments in biological replicates of TRMT10A knockdown vs. the knockdown control cells. A total of 13,306 common m^6A peaks were identified by using exomePeak (58) between TRMT10A knockdown and control cells. Consistent with previous studies, the most common m^6A

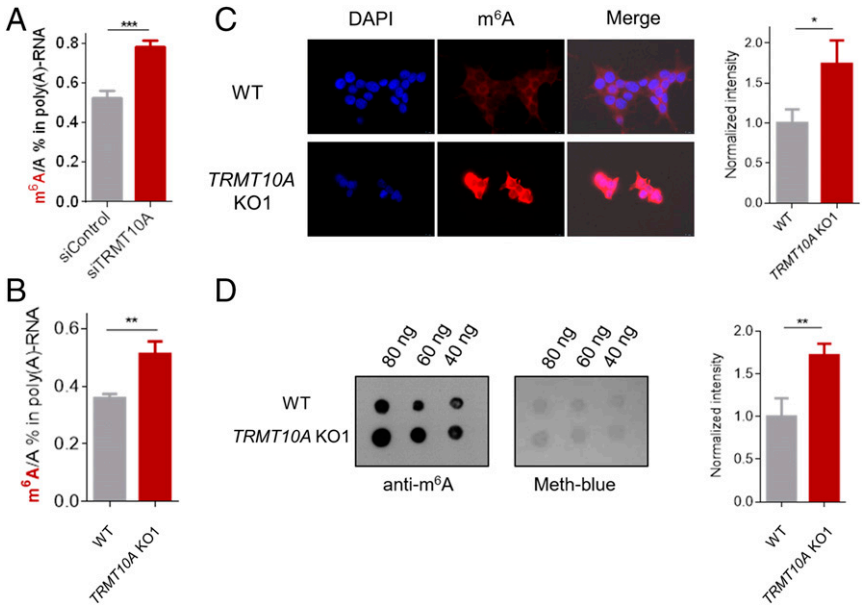

Fig. 2. TRMT10A negatively influences m^{6}A levels in polyadenylated RNA. (*A*) LC-MS/MS showing that knockdown of TRMT10A led to increased m^{6}A/A in polyadenylated RNA in comparison to the knockdown control. (*B*) LC-MS/MS showing that *TRMT10A* knockout led to increased m^{6}A/A in polyadenylated RNA in comparison to the wild-type cells. (*C*) m^{6}A immunostaining (red) of *TRMT10A* knockout (KO) and the wild-type cells, respectively. Nuclei were stained with DAPI. The error bars showing the integrated signals from each cell in the image quantified by ImageJ. (Magnification: 63×.) (*D*) Dot blot analysis of polyadenylated RNA isolated from *TRMT10A* knockout and the wild-type HEK 293T cells. Signals of m^{6}A levels in the immunofluorescence and the dot blot assays were quantified by ImageJ. *P* values were determined using a two-tailed Student's *t* test for unpaired samples. Error bars represent mean ± SD, $n = 8$ (four biological replicates × two technical replicates) for LC-MS/MS samples and $n = 3$ for dot blot samples. *$P < 0.05$, **$P < 0.01$, ***$P < 0.001$.

consensus motif, GGAC (the bold, underlined A is the potential methylated adenosine [m^{6}A]), was significantly enriched in our identified m^{6}A peaks (Fig. 3*A*). After a thorough survey of the individual peaks, we found that a total of 1,344 peaks exhibited a significant increase in m^{6}A levels ($P < 0.05$; $\log_2$ fold-change > 1), and 673 peaks exhibited a significant decrease in m^{6}A levels in TRMT10A knockdown cells relative to knockdown control cells (Fig. 3*B*). Using qRT-PCR experiments, we validated the m^{6}A levels of three individual targets, including *MYC*, *FOXD1*, and *AUPKAIP1*. Each gene transcript showed a significant increase in m^{6}A, reflecting our sequencing analysis (Fig. 3*C*). We assessed the biological processes and molecular functions of the transcripts with increased m^{6}A sites upon TRMT10A ablation via gene ontology (GO) analysis. GO analysis showed that these transcripts are mostly associated with mRNA processing, regulation of mRNA stability, nucleotide binding, and tRNA binding (Fig. 3*D*).

TRMT10A Ablation Leads to Increased m^{6}A in the Shared mRNA Targets of TRMT10A and FTO. To gain insights into TRMT10A-associated RNAs, we utilized cross-linking and immunoprecipitation, followed by high-throughput sequencing (CLIP-seq) experiments. As shown in the TBE-urea gel analysis of the TRMT10A CLIP, TRMT10A interacted with RNA species (*SI Appendix*, Fig. S14*A*). We subsequently performed high-throughput sequencing of the RNA products obtained from CLIP in biological triplicates. As shown in Fig. 4*A*, TRMT10A shared a significant percentage of common mRNA targets with FTO (Fig. 4 *A* and *B*). The overlapped CLIP targets of FTO and TRMT10A also exhibited an increase in m^{6}A peaks upon TRMT10A knockdown in comparison with the knockdown control (Fig. 4*B*), indicating that TRMT10A potentially influences m^{6}A levels in mRNA through its interaction with FTO. We will refer to these transcripts as FTO–TRMT10A-dependent m^{6}A-containing transcripts. To investigate whether TRMT10A associates with FTO's CLIP sites on a transcriptome-wide scale, we analyzed and compared the transcriptomic distribution of the CLIP binding sites for these two enzymes. The results revealed that FTO is enriched in the vicinity of TRMT10A peaks; in contrast, no significant enrichment to randomly selected peaks were observed for FTO (Fig. 4*C*). As shown in Fig. 4*B* and *SI Appendix*, Fig. S14*B*, we have identified several transcripts—including *MYC*, *FOXD1*, and *AURKAIP1*—that exhibited significant m^{6}A enrichment upon TRMT10A knockdown. These same m^{6}A enrichment sites are also concordant with nearby FTO and TRMT10A CLIP sites (Fig. 4*B*). *HPRT1*, which is not a CLIP target of either FTO or TRMT10A, is shown as the negative control.

Shared mRNA Targets of TRMT10A and FTO Are Subjected to Accelerated mRNA Decay Possibly through YTHDF2 in an m^{6}A-Dependent Manner. Next, we searched for the reader proteins working in the same functional axis as FTO and TRMT10A. There are two major families of m^{6}A reader proteins known to specifically recognize m^{6}A in polyadenylated RNAs and bridge the m^{6}A-containing transcripts to the relevant cellular machinery; the YTH proteins and IGF2BP proteins (43, 59). Interestingly, these m^{6}A readers can similarly bind m^{6}A but elicit distinct molecular and biological consequences. YTHDF2 specifically recognizes m^{6}A-containing transcripts and decreases the half-life of the m^{6}A-containing transcripts in comparison to non-methylated ones (26). In contrast, IGF2BP proteins stabilize m^{6}A-containing transcripts (43). Here, we sought to identify the main reader protein that bridges the targeted TRMT10A and FTO-dependent m^{6}A-containing transcripts to cellular effects. Toward this end, we carried out a luciferase reporter assay with insertion of either a wild-type or mutant 3′-UTR of the *MYC* gene. *MYC* was shown as a target in our TRMT10A CLIP-seq, and the m^{6}A level of *MYC* gene increased upon TRMT10A knockdown in comparison to the control as revealed in the m^{6}A-seq results data (Fig. 4*B*). The wild-type form of this reporter transcript has been previously reported as a target for YTHDF2-mediated decay (26). In the mutated reporter transcript, each GGAC (m^{6}A motif with the potentially methylated adenosine bolded and underscored) consensus sequence is changed to

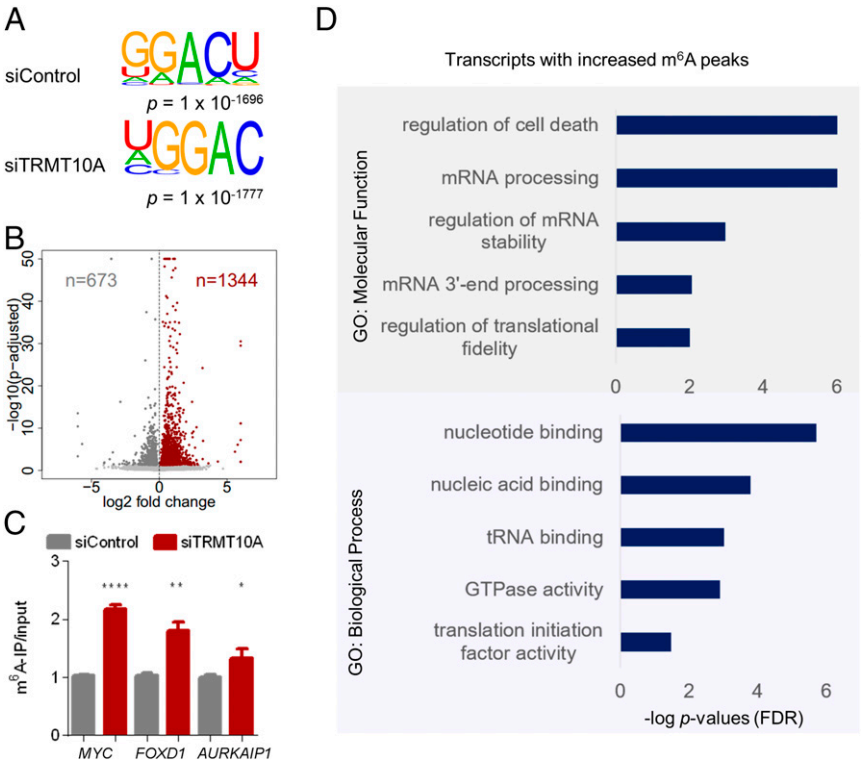

Fig. 3. Transcriptome-wide m^{6}A sites under the regulation of FTO and TRMT10A. (*A*) Sequence logo representing the consensus motifs of two biological replicates of m^{6}A-seq in TRMT10A knockdown and the knockdown control cells. (*B*) Numbers of peaks with increased m^{6}A intensity (red dots) and decreased m^{6}A intensity (gray dots). (*C*) m^{6}A-IP-qRT-PCR showed increased m^{6}A in *MYC*, *FOXD1*, *and AURKAIPI* upon TRMT10A knockdown in comparison to the knockdown control. (*D*) GO analysis of the transcripts with increased m^{6}A peaks upon TRMT10A knockdown in comparison to the knockdown control. FDR, false discovery rate. *P* values were determined using a two-tailed Student's *t* test for unpaired samples. Error bars represent mean ± SD, $n = 6$ (three biological replicates × two technical replicates). $*P < 0.05$, $**P < 0.01$, and $****P < 0.0001$.

GGCC, effectively preventing adenosine methylation (43). Our results showed that TRMT10A knockdown led to decreased luciferase activity and mRNA levels in the wild-type reporter but not in the mutant reporter (Fig. 4*D*). This phenomenon aligned with the known functions of YTHDF2 in accelerating mRNA decay instead of the stabilizing effect of other m^{6}A reader proteins on m^{6}A-containing transcripts (26, 43). In support of this, knockdown of YTHDF2 preferentially increased the half-lives of FTO–TRMT10A-dependent m^{6}A-containing transcripts compared to the nontargeted transcripts (*SI Appendix*, Fig. S15*A*). In contrast, knockdown of IGF2BP1 did not show significant effects on TRMRT10A and FTO-dependent m^{6}A-containing transcripts (*SI Appendix*, Fig. S15*B*). We have also measured the half-lives of a few representatives, m^{6}A-enriched transcripts, including *MYC*, *ATP7A*, *FOXD1*, and *ERCC5*; these transcripts are also the targets of YTHDF2-mediated decay. As shown in Fig. 4*E* and *SI Appendix*, Fig. S16, the half-lives of *MYC*, *ATP7A*, *FOXD1*, and *ERCC5* all decreased in the *TRMT10A* knockout in comparison to the wild-type cells. Knockdown of METTL3 restored the half-life of the three represented genes upon TRMT10A knockdown, which further suggested that the decreased half-lives of these three representative genes upon TRMT10A deficiency are m^{6}A-dependent. Collectively, these results suggest that the complex of FTO and TRMT10A possibly works in the same functional axis with YTHDF2 instead of other m^{6}A reader proteins that stabilize m^{6}A-containing transcripts.

The Catalytic Efficiency of TRMT10A Is not Critical for Its Impact on m^{6}A in Poly(A)-RNA. TRMT10A installs m^{1}G in human and yeast tRNAs (15–17). Consistent with this, *TRMT10A* knockout resulted in a 50% decrease of m^{1}G in total tRNA and TRMT10A knockdown led to a 12% decrease of m^{1}G in total tRNA (Fig. 5*B* and *SI Appendix*, Fig. S17*A*). Reexpression of wild-type TRMT10A (21) led to a rescue of m^{1}G levels in tRNAs, while reexpression of the known catalytic-inactive mutant TRMT10A G206R (21) did not restore m^{1}G levels (Fig. 5*A* and *SI Appendix*, Fig. S18). Interestingly, the reexpression of either the wild-type or G206R TRMT10A variant restores the m^{6}A levels in poly(A)-RNA (Fig. 5*C*). These results suggest that the catalytic activity of TRMT10A is not critical for TRMT10A's impact on m^{6}A in poly(A)-RNA.

To explore the phenotypic effects of TRMT10A deficiency, we next investigated whether TRMT10A deficiency impacts cell proliferation. We observed decreased cell proliferation upon *TRMT10A* knockout in comparison to the wild-type cells; reexpression of either wild-type or G206R TRMT10A variant rescued the impaired cell proliferation elicited by *TRMT10A* knockout. In contrast, expression of empty vector in *TRMT10A* knockout cells failed to repair the cell proliferation defects (Fig. 5*D* and *SI Appendix*, Fig. S19). To study TRMT10A's influence on global protein synthesis, we used an alkyne-modified glycine analog, L-homopropargylglycine (HPG), to metabolically label newly synthesized proteins in *TRMT10A* knockout and wild-type cells, as well as in TRMT10A knockdown versus the knockdown control cells. The HPG-labeled cells were then fluorescently modified and analyzed by flow cytometry. The gating strategy of flow cytometry is shown in *SI Appendix*, Fig. S20. The results showed that TRMT10A ablation did not induce a notable impact on global protein synthesis rate (*SI Appendix*, Fig. S21*A*). In addition, TRMT10A ablation did not alter the protein levels of m^{6}A methyltransferase METTL3 (*SI Appendix*, Fig. S21*B*). These data collectively suggest that TRMT10A is less likely to influence m^{6}A levels in poly(A)-RNA through influencing

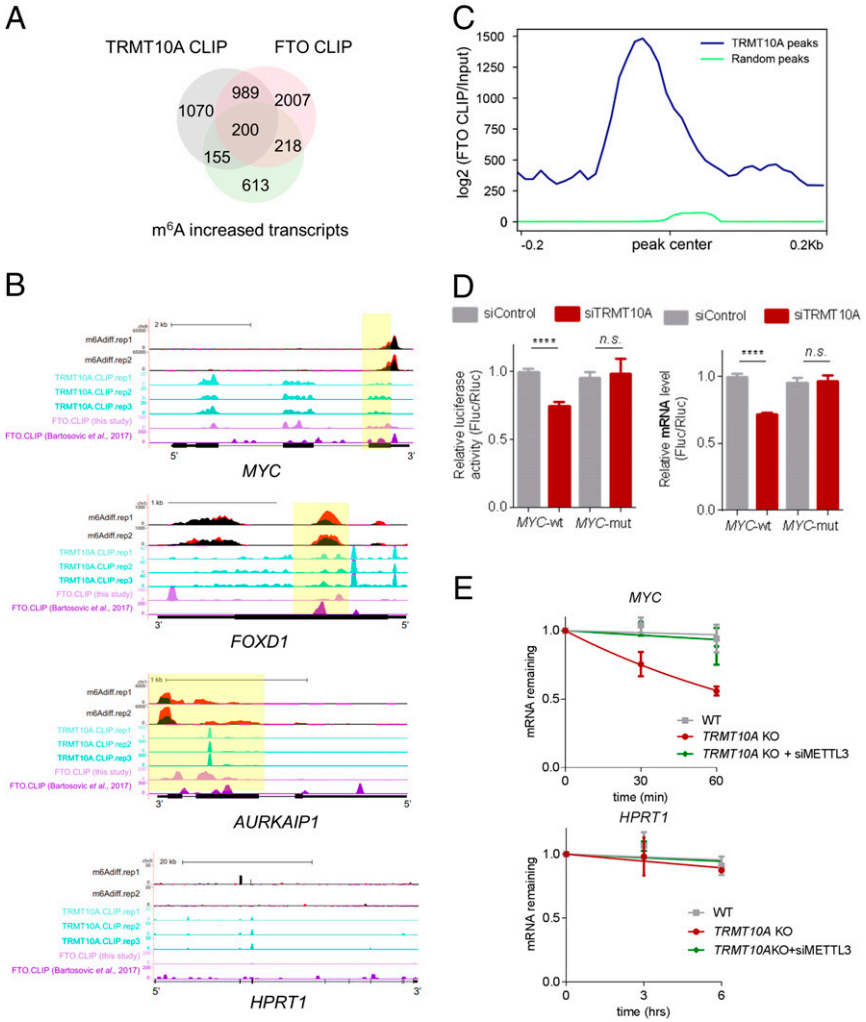

Fig. 4. TRMT10A knockdown led to increased m^{6}A in the shared mRNA targets of TRMT10A and FTO. (*A*) The overlapped transcripts of FTO-CLIP (pink), TRMT10A-CLIP targets (gray), and the transcripts with increased m^{6}A (light green). (*B*) Representative CLIP targets of FTO and TRMT10A, are present with increased m^{6}A peak intensity upon TRMT10A knockdown in comparison to the knockdown control. *HPRT1*, which is not an overlapped CLIP target of FTO and TRMT10A, is present with unaltered m^{6}A peak intensity upon TRMT10A knockdown in comparison to the knockdown control. m^{6}A-IP-seq datasets obtained in knockdown control are shown in black, while the ones obtained in TRMT10A knockdown samples are shown in red. TRMT10A-CLIP datasets are shown in cyan. FTO-CLIP datasets are shown in purple. The light-yellow boxes indicate the overlapped peaks. (*C*) Plots of average binding of FTO per-base around TRMT10A binding sites (blue curve) and random sites (green curve). (*D*, *Left*) relative luciferase activity of *MYC* CRD-wt or *MYC* CRD-mut reporters in TRMT10A knockdown and the knockdown control cells, respectively; (*Right*) qRT-PCR results of *MYC* CRD-wt or *MYC* CRD-mut reporters in TRMT10A knockdown and the knockdown control cells, respectively. (*E*) *MYC*, one overlapped CLIP-target of FTO, and TRMT10A showed decreased half-life time in *TRMT10A* knockout in comparison to the wild-type cells. *HPRT1*, which is not a CLIP targets of either FTO or TRMT10A, was shown as the negative control. *P* values were determined using a two-tailed Student's *t* test for unpaired samples. Error bars represent mean ± SD, $n = 6$ (three biological replicates × two technical replicates). ****$P < 0.0001$, *n.s.* represents $P > 0.05$.

the global protein synthesis or the expression levels of m^{6}A methyltransferase METTL3.

TRMT10A Enhances FTO's m^{6}A Demethylase Activity In Vitro and May Facilitate FTO's Substrate Selectivity Inside Cells. To better understand how FTO is affected by TRMT10A deficiency, we sought to quantify how well FTO binds to its putative mRNA targets. To this end, we performed FTO-CLIP-qRT-PCR on two FTO-targeted mRNAs in both wild-type and *TRMT10A* knockout cells. The results showed that the enrichment ratio of FTO-CLIP versus the vector-CLIP on *MYC* and *FOXD1* was significantly lower in the *TRMT10A* knockout cells relative to the enrichment ratio in the wild-type cells, indicating that TRMT10A facilitated FTO targeting to the correct m^{6}A sites in mRNA (Fig. 6*A*). Furthermore, we performed biochemical assays to measure the m^{6}A demethylase activity of FTO on poly(A)-RNA in the presence and absence of TRMT10A. As shown in Fig. 6*B*, the demethylation activity of FTO is enhanced by approximately threefold in the presence of TRMT10A (at 1:1 molar ratio) in vitro. Similarly, such an in vitro enhancement of FTO's m^{6}A demethylation activity in the presence of TRMT10A was also seen when we used an m^{6}A-containing probe (Fig. 6*C*). Leveraging these in vitro results, we employed a tether assay to further study whether TRMT10A could impact m^{6}A levels in reporter transcripts inside of cells. As shown in the schematic in Fig. 6*D*, we fused wild-type TRMT10A with a λ-peptide; we also added 5-BoxB sequences downstream of the wild-type or mutant (mut) *MYC* CRD domain-containing Firefly luciferase reporters. The results revealed decreased m^{6}A levels in the wild-type CRD Firefly luciferase in comparison to the *MYC* mutant CRD variant luciferase gene in the cells expressing λ-TRMT10A but not the cells expressing only λ-peptide (without TRMT10A fusion).

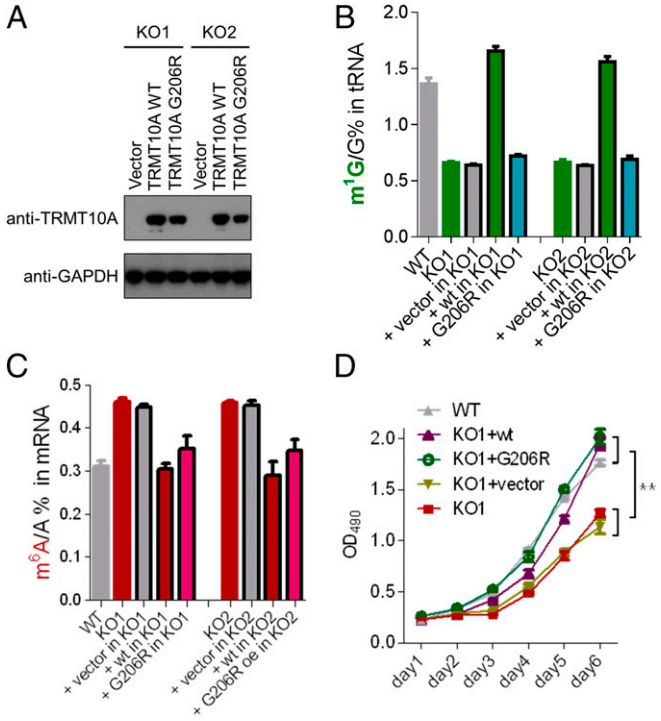

Fig. 5. The catalytic activity of TRMT10A is not critical for its impact on m^6A levels in poly(A)-RNA. (*A*) Western blot showing the reexpression of an empty vector, wild-type TRMT10A, and TRMT10A G206R variant in two *TRMT10A* knockout (KO) single colonies. LC-MS/MS quantification showing that (*B*) *TRMT10A* knockout led to a significant decrease of m^1G level in tRNA. Reexpression of wild-type TRMT10A but not TRMT10A G206R variant led to an increase of m^1G in comparison to cells with TRMT10A ablation. (*C*) *TRMT10A* knockout led to a significant increase of m^6A level in poly(A) RNA. Reexpression of either wild-type TRMT10A or TRMT10A G206R variant but not the empty vector restores the m^6A levels in the wild-type HEK 293T cells. Error bars represent mean ± SD, $n = 6$ (three biological replicates × two technical replicates). (*D*) Cell proliferation assays performed in the wild-type, *TRMT10A* knockout, *TRMT10A* knockout with reexpression of wild-type TRMT10A, *TRMT10A* knockout with reexpression of TRMT10A G206R variant, *TRMT10A* knockout with reexpression of an empty vector HEK293T cells. Error bars represent mean ± SD, $n = 9$ (three biological replicates × three technical replicates). $^{**}P < 0.01$.

These results showed that tethering of TRMT10A to a reporter mRNA containing m^6A target site leads to its demethylation. Collectively, these results suggest that TRMT10A may enhance FTO's demethylation activity and selectivity on m^6A sites in poly(A)-RNA.

FTO-TRMT10A–Dependent m^6A-Containing Transcripts Are Enriched in Codons Corresponding to m^1G9-Containing tRNAs. All of the data collectively intrigued us enough that we were prompted to further study the functional implications of a potential coregulation of modifications in mRNA and tRNA mediated by FTO and TRMT10A. Toward this end, we examined the usage of specific codons in the coding sequences of FTO–TRMT10A-dependant m^6A-containing mRNAs. Each mRNA was analyzed to obtain frequencies of codons corresponding to two categories of tRNAs: 18 m^1G9-tRNAs and 24 tRNAs without m^1G9 (12). The frequency of each codon from this subset of mRNAs was compared to the latest human transcriptome codon frequencies (60) to generate a codon usage bias (Fig. 6*E*). The codons corresponding to $tRNA^{Gln(TTG)}$, $tRNA^{Arg(CCG)}$, and $tRNA^{Thr(CGT)}$, and three m^1G9-containing tRNAs, exhibited the greatest degree of positive usage bias in our set of mRNA transcripts compared to the whole transcriptome (Fig. 6*E*). Together, these data provide the first hints of a concerted regulation of methylation status of m^1G in tRNA and m^6A in mRNA by TRMT10A through its catalytic-dependent and -independent activity. It has been shown that m^6A at any position in a given codon can negatively impact translation-elongation dynamics such that the overall production rate and folding of nascent peptides may be altered (61). In the context of the FTO–TRMT10A complex, it stands to reason that the increased stability of FTO-mediated demethylated mRNAs may be positively coupled with favorable translation dynamics, and perhaps TRMT10A-mediated tRNA methylation supports the translation of these specific transcripts even more.

Discussion

Based on previous work and this study, we summarized a previously unknown mechanism by which the interaction between two distinct RNA modifying enzymes contributes to the dynamic regulation of modifications on mRNAs. Our work shows that a tRNA methyltransferase, TRMT10A, interacts with an mRNA demethylase, FTO, in vitro, inside cells, and in situ. Under normal conditions, TRMT10A facilitates the substrate selectivity and enhances the m^6A demethylase activity of FTO to target and remove the correct m^6A sites in mRNA, thus stabilizing the now unmodified mRNAs. Collectively, TRMT10A maintains a balanced pool of functional tRNAs through its catalytic activity while also influencing mRNA stability and possibly coordinating transcript decoding through its interaction with FTO.

The Interaction of FTO and TRMT10A. Our studies revealed that TRMT10A directly interacts with FTO in an RNA-facilitated manner both in vitro and inside cells. It is an interesting finding considering the opposite enzymatic activities of these two enzymes on very different types of RNA substrates. Moreover, our CLIP-seq data show that FTO and TRMT10A share a significant overlap of CLIP targets, suggesting these two enzymes are spatially near the same set of mRNA targets inside of cells. The overlapped targets participate in a wide array of metabolic pathways related to energy metabolism regulation. This interaction between FTO and TRMT10A was revealed critical to the transcriptome-wide m^6A profile of polyadenylated RNA species, as evidenced by m^6A-seq experiments in TRMT10A knockdown and the knockdown control samples.

Previous studies showed G206R, which is a catalytic-inactive variant of TRMT10A, is present in patients with young onset diabetes and primary microcephaly (22). Interestingly, a few other disease-related mutation sites in TRMT10A are found outside of the catalytic domain and are clustered more toward the N-terminal domain (19, 62). Data from TCGA database highlights several mutation sites in TRMT10A both inside and outside the catalytic domain of TRMT10A from colorectal cancer patients (63, 64). It will be interesting to study and compare the individual effects of mutations to catalytic residues of TRMT10A as opposed to mutations outside the catalytic regions, and how these may be linked to the disease phenotype. Thus far, the interface and structural interactions among FTO, TRMT10A, and the associated RNAs are not yet revealed. It is not known whether specific RNA species functions as a docking site to facilitate the multivalent binding of FTO and TRMT10A to distinct locations, or if the RNA strengthens and solidifies the direct interactions between FTO and TRMT10A at the m^6A site, which should be explored in the future study.

The Dual Functions of tRNA-Modifying Proteins. There is precedent for enzymes, and specifically tRNA-modifying enzymes, to exhibit essential secondary roles that are uncoupled from their canonical catalytic activity. For example, the tRNA m^5U_{54} methyltransferase TrmA is essential for *Escherichia coli* viability yet the presence of its enzymatic product m^5U_{54}-tRNA is not

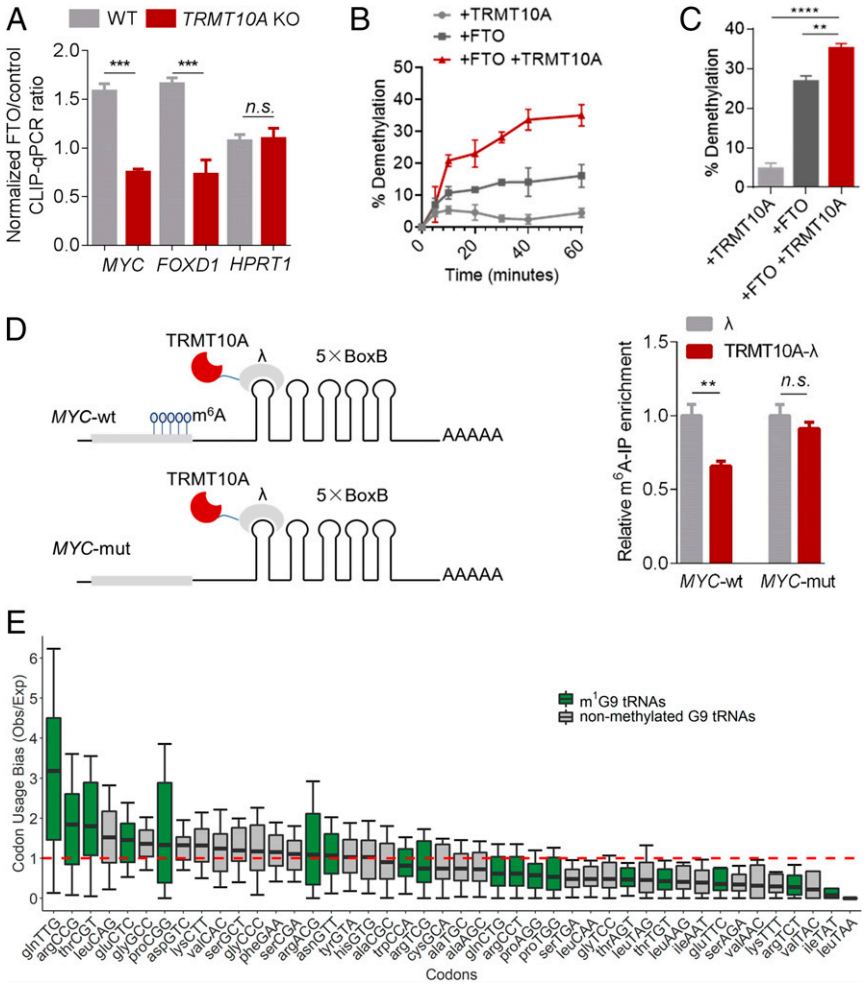

Fig. 6. TRMT10A may facilitate the activity and selectivity of FTO on the m^{6}A in poly(A)-RNA. (*A*) FTO CLIP-qRT-PCR results on *MYC*, *FOXD1*, and *HPRT1* in *TRMT10A* knockout and the wild-type HEK 293T cells. (*B*) LC-MS/MS quantification of m^{6}A levels in poly(A)-RNA extracted from HEK 293T cells after in vitro demethylation reaction with TRMT10A alone (light gray), FTO alone (dark gray), and a mixture of TRMT10A and FTO (red) for different time intervals as shown in the figure. (*C*) LC-MS/MS quantification of m^{6}A levels in an m^{6}A-containing RNA probe after in vitro demethylation reaction with TRMT10A alone (light gray), FTO alone (dark gray) and a mixture of TRMT10A and FTO (red) for 20 min. α-Ketoglutarate was supplemented in all of the in vitro demethylation activity assay. (*D*) The schematic of the tethering assay. TRMT10A was fused with λ protein, which can recognize and bind to 5BoxB sequence, and 5BoxB was added at the 3′UTR of the *MYC*-wt and *MYC* mutant (mut) reporter. Tethering TRMT10A-λ to the 5BoxB-containing *MYC*-wt mRNA reporter led to an ∼35% reduction of the enrichment of m^{6}A in the *MYC*-wt mRNA reporter compared to tethering λ alone. Tethering TRMT10A-λ to the 5BoxB-containing *MYC* mutant mRNA reporter led to nonobvious changes of the enrichment of m^{6}A in the *MYC* mutant mRNA reporter in comparison to tethering λ alone. *P* values were determined using a two-sided Student's *t* test for paired samples. Error bars represent mean ± SD, $n = 6$ (three biological replicates ± two technical replicates). $^{**}P < 0.01$, $^{***}P < 0.005$, $^{****}P < 0.001$, and *n.s.* represents $P > 0.05$. In *E*, codon usage bias (observed frequency/expected frequency) for codons corresponding to either m^{1}G9-containing tRNAs (green) or nonmethylated G9 tRNAs (gray). The black line in each boxplot represents the median of each distribution. The red dashed line represents a null bias. Outliers beyond twice the interquartile range of the data are not shown.

(65). Moreover, the *E. coli* tRNA pseudouridine synthase TruB supports cellular fitness under stress by acting as a tRNA chaperone, even when catalytically inactive (66). These discoveries align with this work to suggest the notion of catalytic-dependent and -independent dual functions of tRNA-modifying enzymes. This dual functionality of tRNA-modifying proteins conserved from bacteria to mammals may help to explain why noncatalytic mutation can still lead to distinct physiological consequences.

The Interplay Between mRNA and tRNA through the Coordination of Modifications. tRNA deciphers the information encrypted in mRNA during translation. The synonymous codons are translated at different speeds primarily determined by the levels of the tRNAs as well as the anticodon–codon pairing between the tRNA and mRNA (67, 68). It is known that tRNA modifications influence the stability of the tRNA molecules and thus impact the level of tRNA inside cells (1, 10, 69). In addition, modification at the anticodon region affects the paring with the mRNA codon. Thus, the overall composition of tRNA pools and their mRNA decoding capacity are heavily influenced by the modification status. Modifications to mRNA impact nearly every step in mRNA processing, including mRNA stability and occupancy in ribosomes, and thus RNA modifications play a significant regulatory role in the functional transcriptome and proteome of a cell (2, 70)

The concurrent existence of mRNA and tRNA modifications is well studied, but how the cell coordinates the modification status of mRNA and tRNA to achieve the desired levels of each of RNA remains a mystery. It is known that many RNA-modifying enzymes can install the same modification in different RNA species (54, 71–74). These modifications perform

similar roles in different RNA species, which indicates that these enzymes may coordinate different RNA species to support cellular events cooperatively. However, due to the overlapped enzyme activity at different RNA substrates, it is not a trivial task to study the individual and collaborative roles of the RNA modifications in different RNA species. FTO and TRMT10A have distinct enzymatic activities and work on two distinct RNA species. Our work reveals that TRMT10A, beyond its catalytic activity, also influences m^6A in mRNA through the interaction with FTO to possibly coordinate the methylation status between mRNAs and tRNAs.

Interestingly, our exploration of the codon composition present in the subset of transcripts regulated by FTO and TRMT10A provides hints that codons corresponding to m^1G-modified tRNAs may be preferentially utilized by this transcript pool. It is an intriguing idea that will warrant further study. Our analysis also yielded several codons that are not significantly enriched or are anticorrelated with our specific transcript pool, including some m^1G-modified tRNAs. It is not entirely surprising that only a subset of m^1G-modified tRNA would be preferentially utilized by this transcript pool, given that other regulatory mechanisms may exist in parallel. It will be interesting to study if this is a general mechanism by which RNA modification statuses are coordinated by functional interactions formed between RNA-modifying enzymes. Beyond just FTO, TRMT10A also interacted with several m^6A reader proteins; the functional significance of these interactions is worthy of future study.

A New Axis of m^6A Interpretation. Transcriptome-wide examination of m^6A coupled with RNA-sequencing data enabled a broad classification of genes subject to FTO–TRMT10A complex control. As evidenced by this classification, the activity and downstream readout of the complex are highly diverse. This likely reflects the diversity in recognition and interpretation by reader proteins. The expression and localization of reader proteins are subject to cell-type specificity as well as temporal control, so any given change in the gene expression of m^6A-containing transcripts is subject to an additional layer of control and complexity at the reader level (27, 38, 42, 43). With this context specificity in mind, comparison and annotation of CLIP-seq RNA targets of both FTO and TRMT10A with m^6A-seq data revealed that FTO and TRMT10A work as a complex in the dynamic regulation of m^6A profile in mRNA. These findings represented one mechanism by which the methyltransferase TRMT10A influences m^6A demethylation through working with FTO, which adds a new layer of regulation of m^6A-mRNA profiles by tRNA-modifying enzymes. FTO has a wide range of substrates. Recent studies suggested that the substrate selectivity is dependent on the cellular localization of FTO (37). We propose that the binding partners of FTO are critical to determining the substrate selectivity and enzymatic activity of this mRNA demethylase. In its functional axis with TRMT10A, we suggest that FTO works on m^6A rather than other m^6A_m in polyadenylated RNA. Although we do not exclude the possibility that under different circumstances and in conjunction with other protein networks, FTO would be more favorably positioned at the mRNA cap modification site.

A question that remains to be answered in the future studies is how m^6A sites are correctly interpreted by reader proteins, especially considering that several reader proteins appear to enact different or opposite cellular functions while still only recognizing the same chemical modification. We propose that the association of FTO and TRMT10A and their collaborative targeting of a specific subset of m^6A-containing mRNAs is a determinant in YTHDF2-mediated decay. Our findings, presented here, open the door for detailed mechanistic studies of FTO and TRMT10A association and biological consequences.

Materials and Methods

Experimental procedures for cloning, expression, and purification of wild-type and mutant TRMT10A and FTO, knockdown of TRMT10A, knockout of *TRMT10A*, polyadenylated RNA isolation, FTO demethylation activity assays, LC-MS/MS quantification of RNA modifications, immunoprecipitation, PLA assays, codon usage analysis, and statistical analysis are described in *SI Appendix, Materials and Methods*.

Data Availability. Sequencing data, including TRMT10A-CLIP seq, FTO-CLIP seq, and m^6A-seq have been deposited into the Gene Expression Omnibus (GEO) under accession number GSE146207.

ACKNOWLEDGMENTS. We thank Drs. Jeremy Wilusz, Kristen Lynch, and Mr. Michael Owens for the constructive discussions and editing this manuscript; and Dr. Jianjun Chen's group for sharing with us the Myc CRD-wt or Myc CRDmut reporters. Research reported in this publication was supported by the National Institute of General Medical Sciences of the National Institutes of Health under grant number R35GM133721.

1. T. Pan, Modifications and functional genomics of human transfer RNA. *Cell Res.* **28**, 395–404 (2018).
2. C. J. T. Lewis, T. Pan, A. Kalsotra, RNA modifications and structures cooperate to guide RNA-protein interactions. *Nat. Rev. Mol. Cell Biol.* **18**, 202–210 (2017).
3. M. Helm, Y. Motorin, Detecting RNA modifications in the epitranscriptome: Predict and validate. *Nat. Rev. Genet.* **18**, 275–291 (2017).
4. S. Li, C. E. Mason, The pivotal regulatory landscape of RNA modifications. *Annu. Rev. Genomics Hum. Genet.* **15**, 127–150 (2014).
5. R. Desrosiers, K. Friderici, F. Rottman, Identification of methylated nucleosides in messenger RNA from Novikoff hepatoma cells. *Proc. Natl. Acad. Sci. U.S.A.* **71**, 3971–3975 (1974).
6. R. C. Desrosiers, K. H. Friderici, F. M. Rottman, Characterization of Novikoff hepatoma mRNA methylation and heterogeneity in the methylated 5′ terminus. *Biochemistry* **14**, 4367–4374 (1975).
7. W. V. Gilbert, T. A. Bell, C. Schaening, Messenger RNA modifications: Form, distribution, and function. *Science* **352**, 1408–1412 (2016).
8. K. E. Sloan *et al*., Tuning the ribosome: The influence of rRNA modification on eukaryotic ribosome biogenesis and function. *RNA Biol.* **14**, 1138–1152 (2017).
9. W. A. Decatur, M. J. Fournier, rRNA modifications and ribosome function. *Trends Biochem. Sci.* **27**, 344–351 (2002).
10. E. M. Phizicky, A. K. Hopper, tRNA biology charges to the front. *Genes Dev.* **24**, 1832–1860 (2010).
11. F. Nau, The methylation of tRNA. *Biochimie* **58**, 629–645 (1976).
12. W. C. Clark, M. E. Evans, D. Dominissini, G. Zheng, T. Pan, tRNA base methylation identification and quantification via high-throughput sequencing. *RNA* **22**, 1771–1784 (2016).
13. A. E. Cozen *et al*., ARM-seq: AlkB-facilitated RNA methylation sequencing reveals a complex landscape of modified tRNA fragments. *Nat. Methods* **12**, 879–884 (2015).
14. C. Cosentino *et al*., Pancreatic β-cell tRNA hypomethylation and fragmentation link TRMT10A deficiency with diabetes. *Nucleic Acids Res.* **46**, 10302–10318 (2018).
15. A. Krishnamohan, J. E. Jackman, Mechanistic features of the atypical tRNA m1G9 SPOUT methyltransferase, Trm10. *Nucleic Acids Res.* **45**, 9019–9029 (2017).
16. W. E. Swinehart, J. C. Henderson, J. E. Jackman, Unexpected expansion of tRNA substrate recognition by the yeast m1G9 methyltransferase Trm10. *RNA* **19**, 1137–1146 (2013).
17. J. E. Jackman, R. K. Montange, H. S. Malik, E. M. Phizicky, Identification of the yeast gene encoding the tRNA m1G methyltransferase responsible for modification at position 9. *RNA* **9**, 574–585 (2003).
18. N. W. Howell, M. Jora, B. F. Jepson, P. A. Limbach, J. E. Jackman, Distinct substrate specificities of the human tRNA methyltransferases TRMT10A and TRMT10B. *RNA* **25**, 1366–1376 (2019).
19. M. Narayanan *et al*.; C4RCD Research Group, Case Report: Compound heterozygous nonsense mutations in TRMT10A are associated with microcephaly, delayed development, and periventricular white matter hyperintensities. *F1000 Res.* **4**, 912 (2015).
20. T. W. Yew, L. McCreight, K. Colclough, S. Ellard, E. R. Pearson, tRNA methyltransferase homologue gene TRMT10A mutation in young adult-onset diabetes with intellectual disability, microcephaly and epilepsy. *Diabet. Med.* **33**, e21–e25 (2016).
21. D. Gillis *et al*., TRMT10A dysfunction is associated with abnormalities in glucose homeostasis, short stature and microcephaly. *J. Med. Genet.* **51**, 581–586 (2014).
22. M. Igoillo-Esteve *et al*., tRNA methyltransferase homolog gene TRMT10A mutation in young onset diabetes and primary microcephaly in humans. *PLoS Genet.* **9**, e1003888 (2013).
23. P. J. Batista *et al*., m(6)A RNA modification controls cell fate transition in mammalian embryonic stem cells. *Cell Stem Cell* **15**, 707–719 (2014).
24. S. Geula *et al*., Stem cells. m6A mRNA methylation facilitates resolution of naïve pluripotency toward differentiation. *Science* **347**, 1002–1006 (2015).

25. X. Wang *et al*., N(6)-methyladenosine modulates messenger RNA translation efficiency. *Cell* **161**, 1388–1399 (2015).
26. X. Wang *et al*., N6-methyladenosine-dependent regulation of messenger RNA stability. *Nature* **505**, 117–120 (2014).
27. W. Xiao *et al*., Nuclear m(6)A reader YTHDC1 regulates mRNA splicing. *Mol. Cell* **61**, 507–519 (2016).
28. I. A. Roundtree *et al*., YTHDC1 mediates nuclear export of N^6-methyladenosine methylated mRNAs. *eLife* **6**, e31311 (2017).
29. J. A. Bokar, M. E. Rath-Shambaugh, R. Ludwiczak, P. Narayan, F. Rottman, Characterization and partial purification of mRNA N6-adenosine methyltransferase from HeLa cell nuclei. Internal mRNA methylation requires a multisubunit complex. *J. Biol. Chem.* **269**, 17697–17704 (1994).
30. J. Liu *et al*., A METTL3-METTL14 complex mediates mammalian nuclear RNA N6-adenosine methylation. *Nat. Chem. Biol.* **10**, 93–95 (2014).
31. S. Schwartz *et al*., Perturbation of m6A writers reveals two distinct classes of mRNA methylation at internal and 5′ sites. *Cell Rep.* **8**, 284–296 (2014).
32. X. L. Ping *et al*., Mammalian WTAP is a regulatory subunit of the RNA N6-methyladenosine methyltransferase. *Cell Res.* **24**, 177–189 (2014).
33. G. Zheng *et al*., ALKBH5 is a mammalian RNA demethylase that impacts RNA metabolism and mouse fertility. *Mol. Cell* **49**, 18–29 (2013).
34. G. Jia *et al*., N6-methyladenosine in nuclear RNA is a major substrate of the obesity-associated FTO. *Nat. Chem. Biol.* **7**, 885–887 (2011).
35. J. Mauer *et al*., Reversible methylation of m^6A_m in the 5′ cap controls mRNA stability. *Nature* **541**, 371–375 (2017).
36. J. Mauer *et al*., FTO controls reversible m^6Am RNA methylation during snRNA biogenesis. *Nat. Chem. Biol.* **15**, 340–347 (2019).
37. J. Wei *et al*., Differential m^6A, m^6A_m, and m^1A demethylation mediated by FTO in the cell nucleus and cytoplasm. *Mol. Cell* **71**, 973–985.e5 (2018).
38. H. Shi *et al*., YTHDF3 facilitates translation and decay of N^6-methyladenosine-modified RNA. *Cell Res.* **27**, 315–328 (2017).
39. C. Xu *et al*., Structural basis for selective binding of m6A RNA by the YTHDC1 YTH domain. *Nat. Chem. Biol.* **10**, 927–929 (2014).
40. H. Shi *et al*., m^6A facilitates hippocampus-dependent learning and memory through YTHDF1. *Nature* **563**, 249–253 (2018).
41. I. Ivanova *et al*., The RNA m^6A reader YTHDF2 is essential for the post-transcriptional regulation of the maternal transcriptome and oocyte competence. *Mol. Cell* **67**, 1059–1067.e4 (2017).
42. M. N. Wojtas *et al*., Regulation of m(6)A transcripts by the 3′→5′ RNA helicase YTHDC2 is essential for a successful meiotic program in the mammalian germline. *Mol. Cell* **68**, 374–387.e12 (2017).
43. H. Huang *et al*., Recognition of RNA N^6-methyladenosine by IGF2BP proteins enhances mRNA stability and translation. *Nat. Cell Biol.* **20**, 285–295 (2018).
44. F. Zhang *et al*., Fragile X mental retardation protein modulates the stability of its m6A-marked messenger RNA targets. *Hum. Mol. Genet.* **27**, 3936–3950 (2018).
45. R. R. Edupuganti *et al*., N^6-methyladenosine (m^6A) recruits and repels proteins to regulate mRNA homeostasis. *Nat. Struct. Mol. Biol.* **24**, 870–878 (2017).
46. J. F. Xiang *et al*., N^6-Methyladenosines modulate A-to-I RNA editing. *Mol. Cell* **69**, 126–135.e6 (2018).
47. T. Chen *et al*., m(6)A RNA methylation is regulated by microRNAs and promotes reprogramming to pluripotency. *Cell Stem Cell* **16**, 289–301 (2015).
48. F. Shen *et al*., Decreased N(6)-methyladenosine in peripheral blood RNA from diabetic patients is associated with FTO expression rather than ALKBH5. *J. Clin. Endocrinol. Metab.* **100**, E148–E154 (2015).
49. Y. L. Weng *et al*., Epitranscriptomic m^6A regulation of axon regeneration in the adult mammalian nervous system. *Neuron* **97**, 313–325.e6 (2018).
50. Y. Wang *et al*., N^6-methyladenosine RNA modification regulates embryonic neural stem cell self-renewal through histone modifications. *Nat. Neurosci.* **21**, 195–206 (2018).
51. C. Zhang *et al*., m^6A modulates haematopoietic stem and progenitor cell specification. *Nature* **549**, 273–276 (2017).
52. A. K. Hopper, R. T. Nostramo, tRNA processing and subcellular trafficking proteins multitask in pathways for other RNAs. *Front. Genet.* **10**, 96 (2019).
53. T. M. Carlile *et al*., mRNA structure determines modification by pseudouridine synthase 1. *Nat. Chem. Biol.* **15**, 966–974 (2019).
54. T. M. Carlile *et al*., Pseudouridine profiling reveals regulated mRNA pseudouridylation in yeast and human cells. *Nature* **515**, 143–146 (2014).
55. S. Schwartz *et al*., Transcriptome-wide mapping reveals widespread dynamic-regulated pseudouridylation of ncRNA and mRNA. *Cell* **159**, 148–162 (2014).
56. L. Han, E. Marcus, S. D'Silva, E. M. Phizicky, *S. cerevisiae* Trm140 has two recognition modes for 3-methylcytidine modification of the anticodon loop of tRNA substrates. *RNA* **23**, 406–419 (2017).
57. C. Chen, B. Huang, M. Eliasson, P. Rydén, A. S. Byström, Elongator complex influences telomeric gene silencing and DNA damage response by its role in wobble uridine tRNA modification. *PLoS Genet.* **7**, e1002258 (2011).
58. J. Meng, X. Cui, M. K. Rao, Y. Chen, Y. Huang, Exome-based analysis for RNA epigenome sequencing data. *Bioinformatics* **29**, 1565–1567 (2013).
59. S. Liao, H. Sun, C. Xu, YTH domain: A family of N^6-methyladenosine (m^6A) readers. *Genomics Proteomics Bioinformatics* **16**, 99–107 (2018).
60. J. Athey *et al*., A new and updated resource for codon usage tables. *BMC Bioinformatics* **18**, 391 (2017).
61. J. Choi *et al*., N(6)-methyladenosine in mRNA disrupts tRNA selection and translation-elongation dynamics. *Nat. Struct. Mol. Biol.* **23**, 110–115 (2016).
62. A. Zung *et al*., Homozygous deletion of TRMT10A as part of a contiguous gene deletion in a syndrome of failure to thrive, delayed puberty, intellectual disability and diabetes mellitus. *Am. J. Med. Genet. A.* **167A**, 3167–3173 (2015).
63. E. Cerami *et al*., The cBio cancer genomics portal: An open platform for exploring multidimensional cancer genomics data. *Cancer Discov.* **2**, 401–404 (2012).
64. J. Gao *et al*., Integrative analysis of complex cancer genomics and clinical profiles using the cBioPortal. *Sci. Signal.* **6**, pl1 (2013).
65. B. C. Persson, C. Gustafsson, D. E. Berg, G. R. Björk, The gene for a tRNA modifying enzyme, m5U54-methyltransferase, is essential for viability in Escherichia coli. *Proc. Natl. Acad. Sci. U.S.A.* **89**, 3995–3998 (1992).
66. L. C. Keffer-Wilkes, G. R. Veerareddygari, U. Kothe, RNA modification enzyme TruB is a tRNA chaperone. *Proc. Natl. Acad. Sci. U.S.A.* **113**, 14306–14311 (2016).
67. C. E. Brule, E. J. Grayhack, Synonymous codons: Choose wisely for expression. *Trends Genet.* **33**, 283–297 (2017).
68. T. E. F. Quax, N. J. Claassens, D. Söll, J. van der Oost, Codon bias as a means to fine-tune gene expression. *Mol. Cell* **59**, 149–161 (2015).
69. C. Lorenz, C. E. Lünse, M. Mörl, tRNA modifications: Impact on structure and thermal adaptation. *Biomolecules* **7**, 35 (2017).
70. I. A. Roundtree, M. E. Evans, T. Pan, C. He, Dynamic RNA modifications in gene expression regulation. *Cell* **169**, 1187–1200 (2017).
71. X. Li *et al*., Base-Resolution mapping reveals distinct m^1A methylome in nuclear- and mitochondrial-encoded transcripts. *Mol. Cell* **68**, 993–1005.e9 (2017).
72. V. Khoddami, B. R. Cairns, Identification of direct targets and modified bases of RNA cytosine methyltransferases. *Nat. Biotechnol.* **31**, 458–464 (2013).
73. S. Hussain *et al*., NSun2-mediated cytosine-5 methylation of vault noncoding RNA determines its processing into regulatory small RNAs. *Cell Rep.* **4**, 255–261 (2013).
74. T. Amort *et al*., Distinct 5-methylcytosine profiles in poly(A) RNA from mouse embryonic stem cells and brain. *Genome Biol.* **18**, 1 (2017).